Cell Reports

APP Metabolism Regulates Tau Proteostasis in Human Cerebral Cortex Neurons

Graphical Abstract

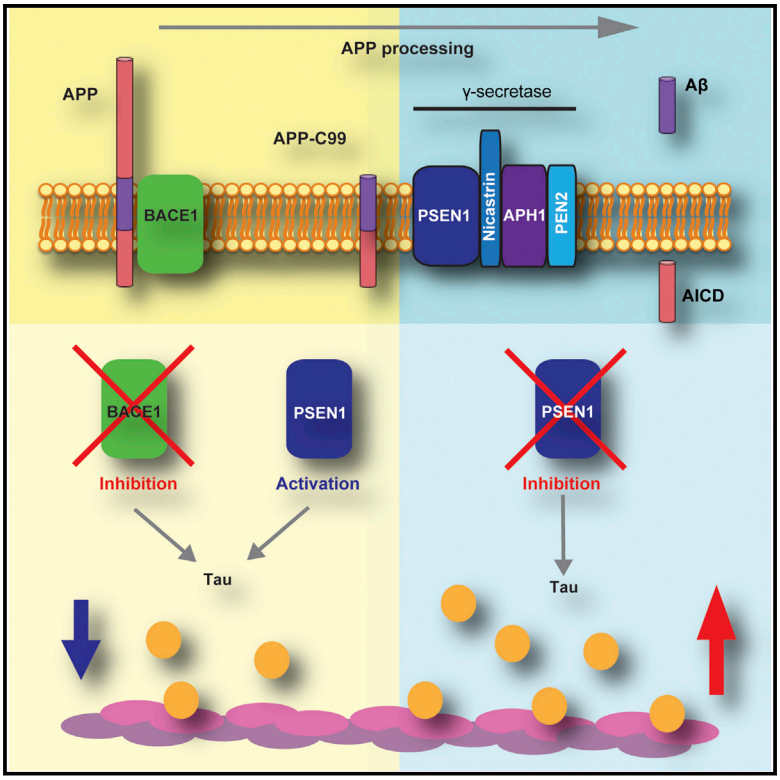

Highlights

- Neurons from different genetic forms of Alzheimer's disease differ in APP processing
- APP mutations increase total and phosphorylated tau; PSEN1 mutations do not
- Pharmacological manipulation of APP processing changes tau protein levels
- APP regulation of tau proteostasis is not solely mediated through extracellular Aβ

Authors

Steven Moore, Lewis D.B. Evans, ..., Henrik Zetterberg, Frederick J. Livesey

Correspondence

rick@gurdon.cam.ac.uk

In Brief

Moore et al. use neurons made from familial Alzheimer's disease stem cells to reveal how three proteins involved in the disease are linked in a pathway that controls disease progression. They show that drugs that target this pathway change levels of a protein involved in neurodegeneration, microtubule-associated protein tau, opening up a potential therapeutic pathway.

Moore et al., 2015, Cell Reports *11*, 689–696
May 5, 2015
http://dx.doi.org/10.1016/j.celrep.2015.03.068

CellPress

Cell Reports
Report

APP Metabolism Regulates Tau Proteostasis in Human Cerebral Cortex Neurons

Steven Moore,[1] Lewis D.B. Evans,[1] Therese Andersson,[2] Erik Portelius,[3] James Smith,[1] Tatyana B. Dias,[1] Nathalie Saurat,[1] Amelia McGlade,[1] Peter Kirwan,[1] Kaj Blennow,[3] John Hardy,[4] Henrik Zetterberg,[3,4] and Frederick J. Livesey[1,*]

[1]The Gurdon Institute, Cambridge Stem Cell Institute and Department of Biochemistry, University of Cambridge, Cambridge CB2 1QN, UK
[2]Department of Molecular Biosciences, The Wenner-Gren Institute, Stockholm University, 106 91 Stockholm, Sweden
[3]Department of Psychiatry and Neurochemistry, Institute of Neuroscience and Physiology, The Sahlgrenska Academy at the University of Gothenburg, 431 80 Molndal, Sweden
[4]Department of Molecular Neuroscience, Institute of Neurology, University College London, Queen Square, London WC1N 1PJ, UK
*Correspondence: rick@gurdon.cam.ac.uk
http://dx.doi.org/10.1016/j.celrep.2015.03.068

SUMMARY

Accumulation of Aβ peptide fragments of the APP protein and neurofibrillary tangles of the microtubule-associated protein tau are the cellular hallmarks of Alzheimer's disease (AD). To investigate the relationship between APP metabolism and tau protein levels and phosphorylation, we studied human-stem-cell-derived forebrain neurons with genetic forms of AD, all of which increase the release of pathogenic Aβ peptides. We identified marked increases in intracellular tau in genetic forms of AD that either mutated APP or increased its dosage, suggesting that APP metabolism is coupled to changes in tau proteostasis. Manipulating APP metabolism by β-secretase and γ-secretase inhibition, as well as γ-secretase modulation, results in specific increases and decreases in tau protein levels. These data demonstrate that APP metabolism regulates tau proteostasis and suggest that the relationship between APP processing and tau is not mediated solely through extracellular Aβ signaling to neurons.

INTRODUCTION

Accumulation of Aβ peptide fragments of the APP protein and neurofibrillary tangles of the microtubule-associated protein tau are the cellular hallmarks of Alzheimer's disease (AD). However, the molecular mechanisms linking APP metabolism; extracellular Aβ peptides; and changes in tau expression, phosphorylation, and cellular localization are currently unclear. Understanding of the genetics underlying monogenic familial Alzheimer's disease (fAD) has provided several insights into disease pathogenesis (Blennow et al., 2006). The majority of known fAD mutations are autosomal dominant and affect *APP* or the catalytic components of the γ-secretase APP-processing complex, presenilin (*PSEN*) 1 and 2 (Bertram and Tanzi, 2008). Early onset AD also occurs in individuals with increased *APP* gene dosage due either to trisomy of chromosome 21 (Ts21) or duplication of the *APP* locus (*APP* (*dup*)) (Rovelet-Lecrux et al., 2006). The identification of the mutations involved in fAD, the discovery of Aβ42 as the primary component of cerebrovascular amyloid (Glenner and Wong, 1984a) and amyloid plaques (Masters et al., 1985) in late-onset sporadic AD, and the identification of the same peptide in amyloid plaques in Down syndrome (Glenner and Wong, 1984b) led to the development of the amyloid hypothesis for AD (Hardy and Allsop, 1991).

The amyloid hypothesis postulates that accumulation of Aβ42 is central to AD initiation and subsequently leads to changes in neuronal function, tau pathology, and ultimately cell death (Hardy and Allsop, 1991). Increased production of aggregation-prone Aβ monomers during AD initiation results in the formation of soluble extracellular oligomers that are proposed to signal via several different specific cell surface receptors or perturb membrane integrity in a non-specific manner, resulting in neuronal dysfunction (Benilova et al., 2012). Changes in APP processing and the generation of intracellular APP fragments have also been proposed to be involved in AD pathogenesis (Pimplikar et al., 2010). The β-secretase-generated C-terminal fragment of APP, referred to as β-CTF or C99, has been shown to be toxic in cultured cells (Yankner et al., 1989) and cause neurodegeneration and defects in synaptic plasticity in transgenic mouse models (Lauritzen et al., 2012). Similarly, cleavage of APP-C99 by γ-secretase releases the APP intracellular domain (AICD), which is proposed to contribute to neurodegeneration (Pimplikar et al., 2010).

We and others have previously shown that neurons generated from induced pluripotent stem cells (iPSCs) from genetic forms of AD recapitulate aspects of the disease, including increased Aβ peptide production in Down syndrome (Shi et al., 2012a) and *APP* duplication (Israel et al., 2012). Altered Aβ40:42 ratios have also been observed in *PSEN1* and *APP* mutant neurons (Muratore et al., 2014; Yagi et al., 2011). Here, we investigate the relationship between APP processing and tau protein levels and phosphorylation by analysis of iPSC-derived cortical neurons with different genetic forms of AD and pharmacological manipulation of β-secretase and γ-secretase.

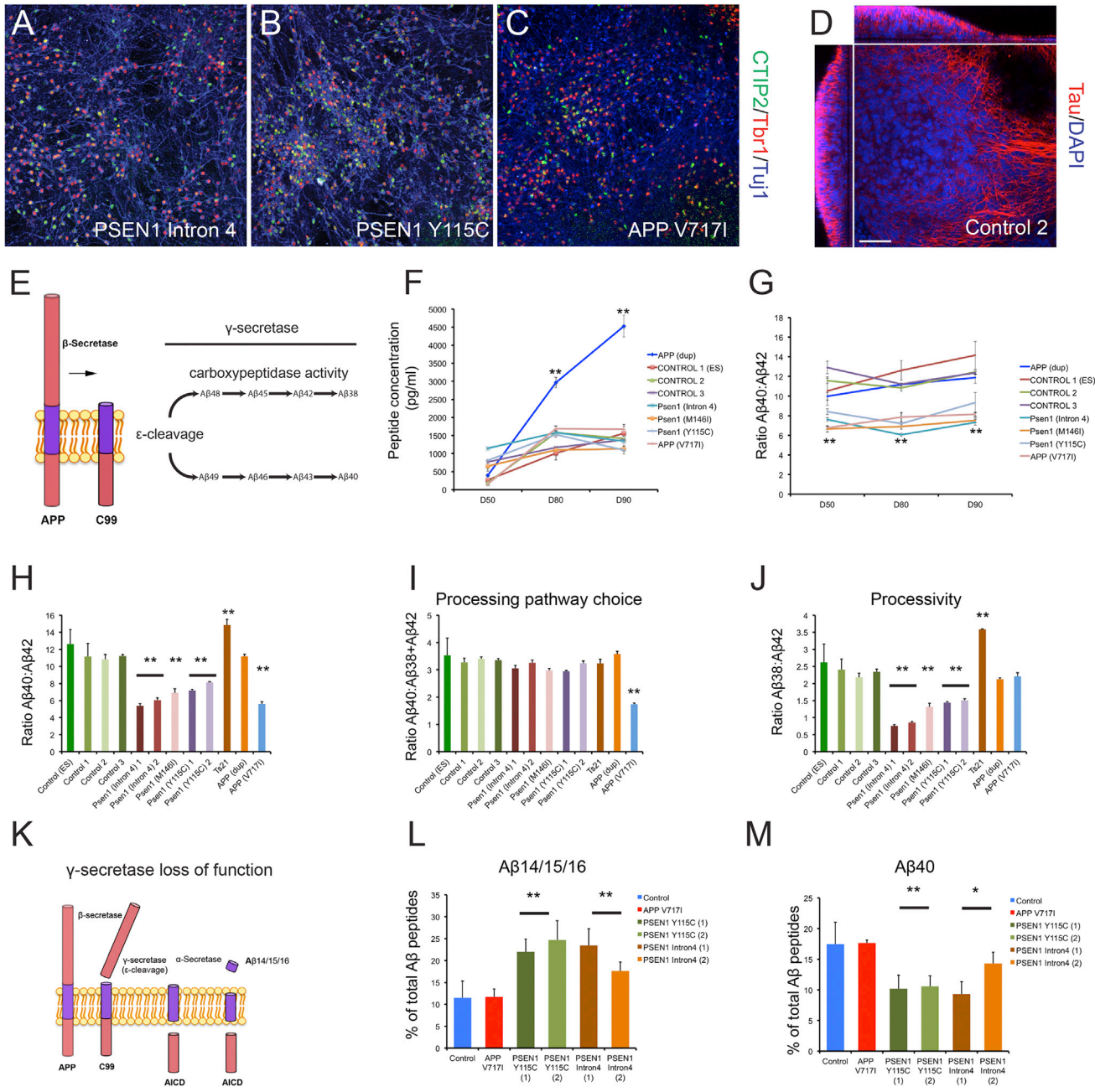

Figure 1. Altered APP Processing and Aβ Peptide Production in Stem Cell Models of Genetic Forms of Alzheimer's Disease

(A–C) Representative immunohistochemistry of neurons (β3-tubulin positive, blue) generated from familial Alzheimer's disease (fAD) (*PSEN1* intron 4, Y115C, and *APP* V717I) iPSCs, expressing transcription factors restricted to layer 6 (Tbr1, red) or layer 5 (CTIP2, green) cortical projection neurons.

(D) 3D nature of stem-cell-derived cortical cultures. Cultures cleared by passive CLARITY and immunostained for neurons (tau, red) and nuclei (DAPI, blue). Single-plane XY, XZ, and YZ (right, top, and left panels, respectively) projections of control neurons 100 days post-induction. The scale bar represents 100 μm.

(E) Generation of Aβ peptides. APP is first cleaved by β-secretase to generate membrane-bound APP-C99. This is followed by the initial γ-secretase cleavage of APP-C99, termed ε-cleavage, to generate Aβ peptides of either 48 or 49 amino acids. Aβ peptides are then subject to sequential γ-secretase carboxypeptidase cleavages, leading to extracellular release of Aβ42, 40 and 38.

(F) Neurons with three different *PSEN1* mutations generate equivalent amounts of total extracellular Aβ peptides over 40 days in culture as three different healthy control lines. *APP* V717I neurons also do not significantly alter the production of total Aβ peptides compared to controls. This is in contrast with *APP* (*dup*) neurons, which significantly increase Aβ production. Error bars, SD; n = 3 cultures for each genotype; $^{**}p < 0.01$.

(G) *PSEN1* and *APP* V717I mutant neurons have significantly reduced Aβ40:Aβ42 ratios compared with both control and *APP* (*dup*) neurons at all time points studied, reflecting a relative increase in the generation of Aβ42. Error bars, SEM; $^{**}p < 0.01$.

(legend continued on next page)

RESULTS

Distinct Genetic Forms of Alzheimer's Disease All Increase Aβ42 Generation

APP processing and generation of Aβ peptides in different genetic forms of AD was studied by generating cortical excitatory neurons from patient iPSCs (Shi et al., 2012c) harboring *PSEN1* mutations (Y115C, M146I, and intron 4), an *APP* mutation (V717I), and APP duplication (APP^{dup}) (Israel et al., 2012; Figures 1A–1C and S1). Over 3 months, neurons generated from monolayers of cortical progenitor cells formed dense 3D, electrically active neural networks that spanned >200 μm in thickness (Figure 1D; Movies S1 and S2).

Production of extracellular Aβ peptides by neurons of each genotype was compared with that of three independent controls over the course of 90 days in culture. At all time points, *PSEN1* and *APP* V717I neurons produced similar extracellular concentrations of the sum of Aβ38, 40, and 42 peptides as healthy control neurons (Figures 1E and 1F). However, these mutants decreased the ratio of Aβ40:Aβ42 at each point assessed (Figures 1F and 1G), reflecting an absolute and relative increase in Aβ42 production compared with controls. In contrast with the other genotypes, APP^{dup} neurons greatly overproduce Aβ peptides over time, in line with increased substrate dosage (Figure 1F), as previously found for Ts21 neurons (Shi et al., 2012a). Overproduction of Aβ peptides in APP^{dup} neurons did not alter the relative amounts of Aβ40 and Aβ42 (Figures 1G and 1H), indicating that Aβ generation is limited by APP availability, rather than β- and γ-secretase capacity.

Comparing relative amounts of Aβ40 with the sum of Aβ38 and Aβ42 peptides enables inference about the initial ε-cleavage of APP-C99 by γ-secretase to either Aβ48 or Aβ49 that are then processed in largely separate pathways (Figure 1E; Chávez-Gutiérrez et al., 2012). *APP* V717I neurons exhibited a significant decrease in the Aβ40:Aβ38+Aβ42 ratio, which was not observed in *APP* dosage models or *PSEN1* mutants (Figure 1I), consistent with the V717I mutation biasing the initial ε-cleavage of APP to Aβ48, which is processed to both Aβ42 and Aβ38 (Figure 1E).

Multiple *PSEN1* mutations resulted in a decreased Aβ38:Aβ42 ratio (Figure 1J), consistent with a hypomorphic loss of γ-secretase function (Chávez-Gutiérrez et al., 2012). In support of this, *PSEN1* mutants significantly increased the release of Aβ14, Aβ15, and Aβ16 (Figures 1K, 1L, and S2), which are thought to be produced by sequential cleavage of APP by β- and then α-secretase in the context of reduced γ-secretase processivity (Portelius et al., 2011). This was accompanied by a reduction in Aβ40, reflecting the shift in production to shorter Aβ forms (Figure 1M), indicating that these hypomorphic *PSEN1* mutations reduce γ-secretase's carboxypeptidase activity.

Increased *APP* Gene Dosage and *APP* V717I Specifically Increase Neuronal Tau Protein Levels

Intracellular levels of total and phosphorylated tau were increased in *APP* V717I and APP^{dup} neurons, compared with controls (Figures 2A, 2C–2E, and S3A; n = 2 independent inductions from each iPSC line). The changes in tau protein levels did not reflect an increase in the relative numbers of neurons carrying APP duplications or mutations, assessed by the levels of the neuron-specific β3-tubulin protein (Figure 2B). Neurons from two different *PSEN1* mutations (Y115C and intron 4) did not exhibit increased total or phosphorylated tau levels, compared to controls (Figures 2A, 2C–2E, and S3A). Thus, intracellular tau levels do not correlate with the extracellular Aβ40:Aβ42 ratio, as *PSEN1* mutant neurons exhibited a comparable ratio to *APP* V717I neurons (Figures 1G and 1H). *MAPT* transcription was assessed by RT-PCR, demonstrating no difference in mRNA expression between neurons of each genotype (Figure S3B) and suggesting that the increase in tau protein observed in *APP* V717I and APP^{dup} neurons is post-transcriptional and a result of altered tau proteostasis.

Pharmacological Manipulation of APP Processing Regulates Tau Proteostasis in Neurons

As *PSEN1* and *APP V717I* mutant neurons displayed strikingly different intracellular tau protein levels but comparable levels of total extracellular Aβ and Aβ40:Aβ42 ratios, we hypothesized that membrane-bound or intracellular products of APP processing might regulate tau proteostasis. Therefore, we compared the effects of acute γ-secretase or β-secretase inhibition on tau protein levels in control neurons. As expected, inhibition of either γ- or β-secretase significantly reduced extracellular Aβ peptides (Figure 3A). However, γ-secretase inhibition led to an increase in tau and a marked accumulation of APP-C83/C99. Tau levels were decreased by β-secretase inhibition (Figure 3B), a treatment that reduces APP-C99 generation. These data indicate a link between APP processing and tau proteostasis that is regulated by γ- and β-secretase activity, independent of extracellular Aβ38, Aβ40, and Aβ42.

(H) *PSEN1* and *APP* V717I mutant neurons exhibit a relative increase in Aβ42 compared to Aβ40 at day 80, whereas Ts21 and *APP* (*dup*) do not. All data produced from three independent cultures. Error bars, SD; $^{**}p < 0.01$.

(I) Comparing ratios of Aβ40 to the sum of Aβ38 and Aβ42 at day 80, as an indicator of ε-cleavage and processing pathway choice, reveals that neither *PSEN1* mutants nor increased *APP* dosage affects APP-C99 cleavage. By contrast, *APP* V717I mutants significantly bias the ε-cleavage APP-C99 to Aβ48, which is processed to both Aβ42 and Aβ38. Error bars, SD.

(J) *PSEN1* mutant neurons have reduced Aβ38:Aβ42 ratios, in contrast with all other genotypes analyzed, suggesting reduced γ-secretase processivity. Error bars, SD; $^{**}p < 0.01$.

(K) Proposed alternative processing pathway of APP in the presence of γ-secretase inhibitors. APP can be sequentially cleaved by β- and then γ-secretase epsilon cleavage followed by α-secretase to generate Aβ14/15/16 and AICD.

(L) Percentage of total Aβ peptides that are generated from the proposed alternative pathway (K; Aβ14/15/16) as an indicator of processivity, detected and quantified by IP-MALDI. *PSEN1* mutant neurons significantly increase the percentage of Aβ peptides made up of the sum of Aβ1-14, 1-15, and 1-16, compared with control and APP V717I neurons. Error bars, SD; $^{**}p < 0.01$.

(M) Percentage of total Aβ peptides that is Aβ40 as an indicator of processivity. *PSEN1* mutant neurons significantly decrease the percentage of Aβ40 peptides, compared with control and APP V717I neurons. Error bars, SD; $^{**}p < 0.01$.

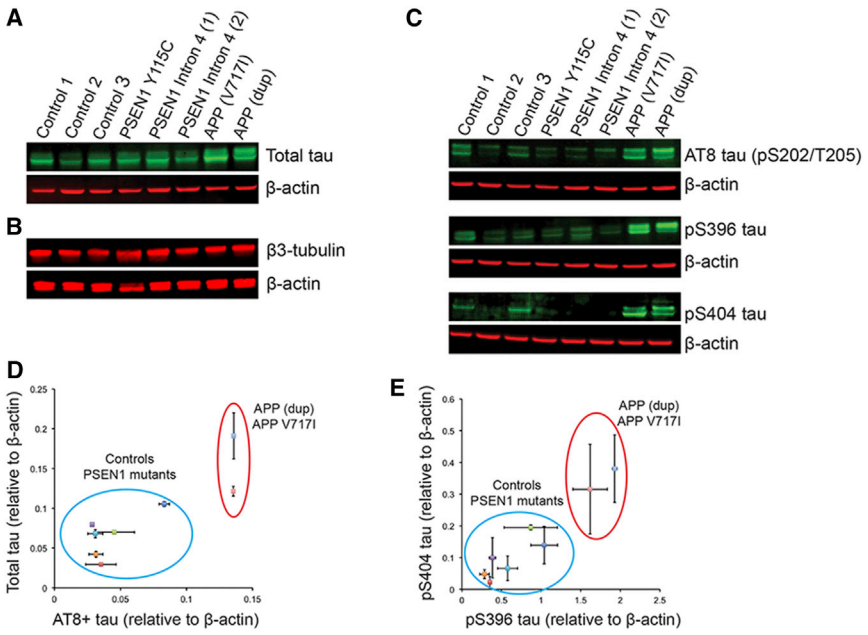

Figure 2. Increased APP Copy Number and the V717I Mutation Lead to Increases in Intracellular Tau Protein Levels, whereas PSEN1 Mutations Do Not

(A) Total tau levels are increased in *APP* (*dup*) and *APP* V717I neurons (90 days post-neural induction) but are not altered in *PSEN1* mutants.

(B) Altered tau levels are not accompanied by changes in neuronal number or mass, assessed by β3-tubulin levels.

(C) Tau phosphorylation at S202/T205, S396, and S404 is increased in *APP* (*dup*) and *APP* V717I neurons, but not *PSEN1* mutants, compared to controls (AT8 and pS396 share actin loading control; for clarity this appears beneath both western blots).

(D and E) Quantification of the data presented in (A), (C), and Figure S3 demonstrating that *PSEN1* mutants do not exhibit increases in tau expression or phosphorylation by western blot analysis. Error bars, SEM.

We compared the effects of the γ-secretase inhibitor (GSI) DAPT with the imidazole-based γ-secretase modulator E2012 (GSM) on Ts21 neurons, which exhibit increased tau protein levels and phosphorylation compared with euploid controls, providing a sensitive background on which to detect changes in tau protein. Ts21 neurons treated with DAPT over a 30-day period exhibited a dose-dependent increase in tau protein levels, accompanied by corresponding increases in APP-C83/C99 (Figures 3C and 3E). However, γ-secretase modulation resulted in a dose-dependent decrease in tau protein levels in Ts21 neurons but did not increase APP-C83/C99 (Figures 3D and 3E).

γ-Secretase Modulation Reduces Intracellular Tau in fAD Neurons

We investigated the effect of manipulating γ-secretase activity on tau proteostasis in different genetic forms of AD. To do so, we compared the effects of γ-secretase inhibition and modulation on APP processing, Aβ peptide production, and tau protein levels in Ts21, *PSEN1*, and *APP* V717I neurons, representing AD initiation due to increased *APP* copy number, reduced γ-secretase carboxypeptidase processivity, and altered ε-cleavage of APP, respectively.

Inhibition of γ-secretase with DAPT significantly reduced the production of extracellular Aβ38, Aβ40, and Aβ42 in neurons of all genotypes (Figures 4A and S4A–S4C; n = 2 independent experiments for each genotype). Moreover, IP-MALDI analysis of extracellular DAPT-treated samples revealed a loss of all longer Aβ peptides and a significant increase in Aβ14, 15, and 16 (Figure S4E). By contrast, E2012 reduced the absolute amount of Aβ40 and Aβ42 in all genotypes assessed and resulted in a marked increase of Aβ37 and Aβ38 (Figures S4A–S4C and S4F), causing increased Aβ40/Aβ42 and Aβ38/Aβ42 ratios for E2012-treated neurons, compared to vehicle controls (Figures 4B and 4C). Notably, E2012 treatment increased Aβ40/Aβ42 and Aβ38/Aβ42 ratios in *PSEN1* mutant neurons, demonstrating that GSMs can act on neurons carrying *PSEN1* mutations. The magnitude of this effect was dependent on the nature of the mutation, with *PSEN1* intron 4 mutations being least responsive to γ-secretase modulation by E2012 (Figures 4A–4D and S4A–S4C).

In agreement with our analyses of control and Ts21 neurons, DAPT increased total tau levels and APP-C83/99 in neurons of all genotypes (Figures 4E, 4F, and S4). This was accompanied by increases in site-specific phosphorylation of tau (pS202/T205 [AT8], pS396, and pS404; Figures 4E and S4E). E2012 significantly reduced tau protein levels and phosphorylation in neurons of each genotype, with the exception of *PSEN1* intron 4 (Figures 4E and S4G). Ts21 neurons, which displayed the most marked changes in APP processing in response to E2012, similarly had the largest increase in both tau protein expression and phosphorylation (Figures 4E and S4G). Given that manipulating γ-secretase could affect neurogenesis and neuronal differentiation via Notch signaling, we measured levels of neuron-specific β3-tubulin in neurons of all genotypes following treatment with GSI and GSM (Figure 4F). Neither drug treatment had any effect on β3-tubulin levels (Figure 4F) and thus did not affect neuronal number or mass.

DISCUSSION

To investigate the relationship between APP metabolism and tau protein levels and phosphorylation, we have utilized human-stem-cell-derived excitatory cortical neurons from representative genetic forms of AD with mutations in either *APP* or *PSEN1* that are predicted to affect APP metabolism. In addition to identifying different classes of altered APP processing and Aβ peptide production under physiological conditions in human forebrain neurons with different genetic forms of AD, we identified regulation of tau proteostasis by metabolism of APP. Marked increases in tau protein levels were observed in genetic forms of AD that changed *APP* dosage or affected the

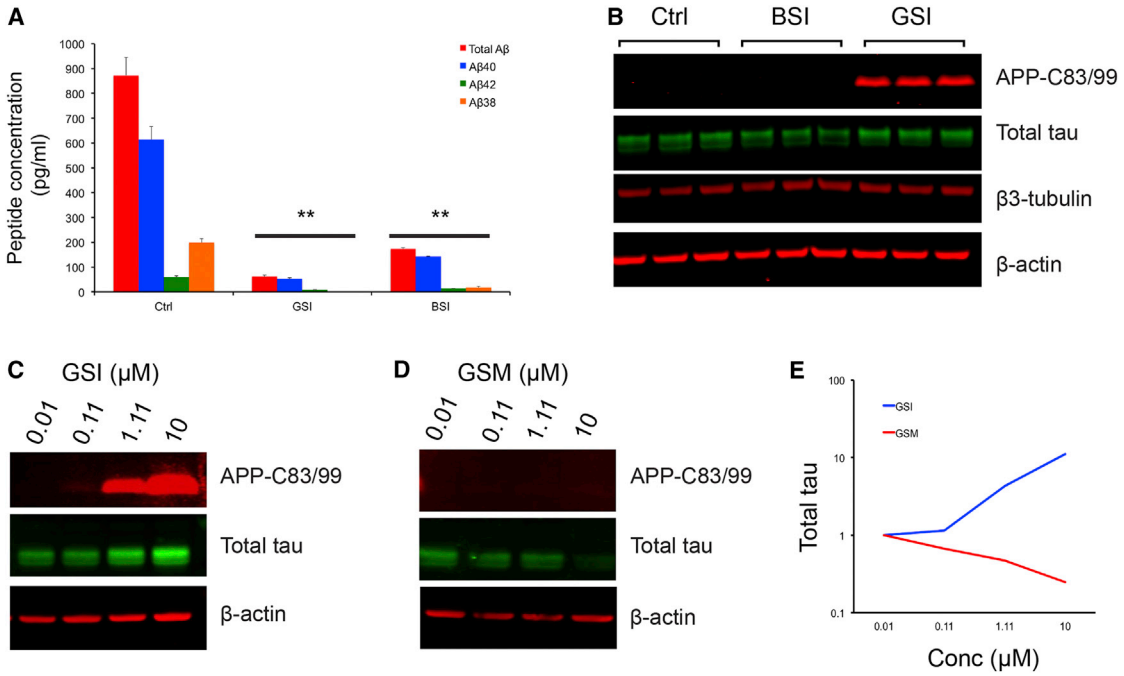

Figure 3. γ-Secretase Processing of APP Is Coupled to Tau Proteostasis

(A) Multiplexed ELISA quantification of extracellular Aβ peptides from healthy control neurons following treatment with the γ-secretase inhibitor, DAPT (GSI), shows significant reduction in the production of Aβ38, Aβ40, and Aβ42, compared to vehicle controls (Ctrl). Similarly, the β-secretase inhibitor LY2886721 (BSI) significantly reduces extracellular Aβ. Neurons treated between days 64 and 70 with the indicated compounds at a final concentration of 1 μM. Error bars, SD. n = 3 cultures for each treatment group; **$p < 0.01$.

(B) Immunoblot detection of APP-C83/99 peptides, total tau, and β3-tubulin extracted from healthy control neurons following treatment with DMSO (Ctrl), BSI, and GSI. BSI treatment reduces tau protein levels with no detectable changes in APP-C83/99, compared to DMSO-treated controls. By contrast, GSI treatment markedly increases both APP-C83/99 and tau in control neurons.

(C–E) Ts21 neurons treated with DAPT (GSI) for a 30-day period between days 60 and 90 post-induction exhibit a dose-dependent increase in both APP-C83/99 and tau protein. Treatment with the γ-secretase modulator E2012 (GSM) reduced tau levels in Ts21 neurons in a dose-dependent manner, with no detectable changes in APP-C83/C99.

ε-cleavage site of APP. Furthermore, pharmacological manipulation of APP metabolism changed tau protein levels in human forebrain neurons in a dose-dependent manner. These findings point to a potentially important pathogenic mechanism in AD, linking APP metabolism to tau protein levels. The pathological significance of tau protein levels is clear from the small number of identified individuals with frontotemporal dementia and *MAPT* duplications (Hooli et al., 2014; Rovelet-Lecrux et al., 2010).

Recent in vitro studies of AD employing overexpression of transgenes encoding mutant forms of *PSEN1* and *APP* in human neurons or iPSC-derived *APP* V717I neurons have demonstrated an association between APP processing and tau pathology that is dependent on extracellular Aβ peptides (Choi et al., 2014; Muratore et al., 2014). Consistent with previous studies, we found that neurons from all fAD lines in this study led to an increase in extracellular Aβ42. However, only *APP* duplication, Ts21, and *APP* V717I resulted in increased tau protein levels and phosphorylation. Elevated tau protein levels were not due to an increase in *MAPT* mRNA expression, suggesting a post-transcriptional mechanism.

Given the similarity in extracellular total Aβ levels and specifically Aβ42, among different *PSEN1* and *APP* mutant neurons, we hypothesized that the increase in intracellular tau protein seen in a subset of genetic forms of AD may be regulated by factors in addition to extracellular Aβ. As the three genotypes in which increased tau occurs either affect total APP levels (Ts21; *APP* duplication) or the initial ε-cleavage of APP by γ-secretase (*APP* V717I), our studies focused on the initial intracellular processing of APP to generate APP-C83/99. Therefore, we compared the effects of β-secretase and γ-secretase inhibition on APP processing and tau proteostasis in human cortical neurons. Both compounds greatly reduce extracellular Aβ peptide production but at different stages of the APP-processing pathway (De Strooper, 2010). β-secretase inhibition prevents generation of APP-C99 from full-length APP, whereas γ-secretase inhibition blocks the proteolysis of APP-C83/99, resulting in accumulation of APP-C83/99. In support of a role for APP metabolism and APP-C83/99 in regulating tau levels, we found that γ-secretase inhibition increased intracellular tau protein levels, whereas β-secretase inhibition reduced intracellular tau protein.

The strategy of γ-secretase modulation reduced tau protein in different genetic forms of AD, suggesting that this approach to reducing tau levels may be a useful therapeutic strategy in different forms of Alzheimer's disease. The reduction in tau

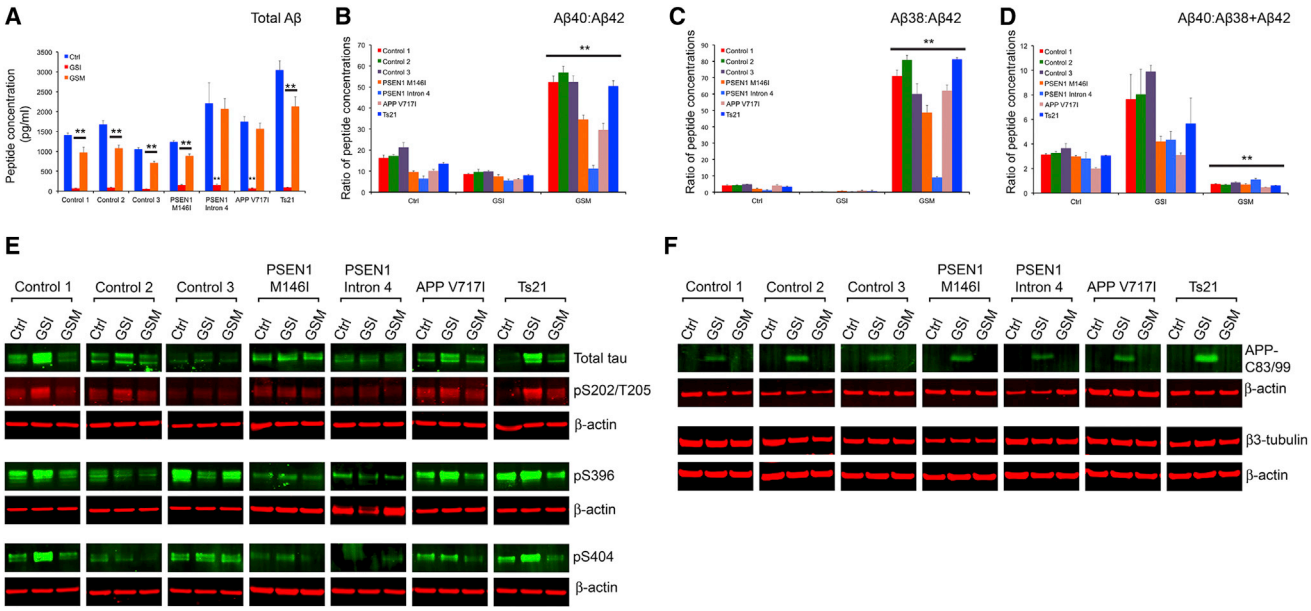

Figure 4. Manipulation of γ-Secretase Activity Alters Aβ Peptide Production, Tau Expression, and Phosphorylation Status in Genetic Forms of AD

(A) DAPT (GSI) prevents the production of Aβ38, Aβ40, and Aβ42 observed in DMSO-treated controls (Ctrl). In contrast, E2012 (GSM) reduces total Aβ peptide production by approximately one third. All compounds used at 1 μM and extracellular media analyzed at day 80 post-neural induction, after 20 days of drug treatment. Error bars, SD. Neurons of each genotype are as marked; n = 3 cultures for each treatment group; $^{**}p < 0.01$.

(B–D) Changes in relative Aβ peptide production in response to each compound are reflected in the ratios between the different Aβ species. E2012 (GSM) has particularly marked effects in reducing the concentration of Aβ42 relative to Aβ40 (B) and in increasing the concentration of Aβ38 relative to Aβ42 (C). Error bars, SD; $^{**}p < 0.01$.

(E) Western blots performed on soluble protein extracts of neurons following treatment with the indicated compounds. Protein extraction performed at day 90 post-neural induction, after 30 days of drug treatment. DAPT treatment (GSI) increases both total and phosphorylated tau expression in the majority of genotypes, assessed at multiple epitopes. By contrast, E2012 (GSM) reduces total tau expression and its phosphorylation in all genotypes assayed, with particularly pronounced effects in Ts21 neurons. Error bars, SD; n = 2 for each treatment group; representative western blots shown, with additional data in Figure S4.

(F) GSI with DAPT increased APP-C83/99 in neurons of all genotypes, with differing efficacy in some *PSEN1* mutants, whereas GSM (E2012) had no effect on APP-C83/99. Drug treatments had no effect on neuronal number, as reflected in the amount of neuron-specific β3-tubulin.

protein by γ-secretase modulation with E2012 had differential effects depending on the specific mutation, with the degree of tau reduction correlated with the magnitude of the change in APP processing in each genotype. For example, E2012 had the most-pronounced effects on APP processing and tau levels in Ts21/Down syndrome neurons and the least effects on both APP processing and tau protein levels in *PSEN1* intron 4 neurons. Finally, γ-secretase modulation also reduced tau protein levels in healthy controls, indicating that the link between APP metabolism and tau proteostasis is a feature of neuronal biology in health and disease.

Overall, our data support a link between APP metabolism and tau proteostasis that is mediated by β- and γ-secretase. The lack of changes in tau protein in *PSEN1* mutant neurons indicates that a simple lack of carboxypeptidase processivity does not lead to altered tau proteostasis. Instead, the data reported here suggest the changes in tau levels are related to altered ε-cleavage of APP by endopeptidase activity of γ-secretase and point to a possible role for APP-C99 in regulating tau proteostasis. A key question for further study is how intracellular metabolism of APP may input into controlling tau proteostasis, given the potential importance of this pathway for AD progression.

EXPERIMENTAL PROCEDURES

Generation of Familial Alzheimer's Disease iPSCs and Cerebral Cortex Neurons

PSEN1 Y115C, M146I, intron 4, and *APP* V717I mutant fibroblasts were sourced as described (Wray et al., 2012). Fibroblasts were reprogrammed at the Cambridge Biomedical Centre using the standard four-factor method, delivered by lentiviruses (Takahashi et al., 2007). Each mutation was sequenced in reprogrammed clones, and pluripotency was determined by differentiation to each germ layer from embryoid bodies (Figure S1). Healthy control cell lines were NDC (Israel et al., 2012), NAS6 (Devine et al., 2011), and the H9 ES (WiCell Research Institute); additional disease lines were *APP* duplication (Israel et al., 2012) and Ts21 iPSCs (Park et al., 2008). Pluripotent cells were cultured by standard methods (see Supplemental Information for details).

Directed differentiation of hESCs and iPSCs to cerebral cortex was carried out as described, with minor modifications (Shi et al., 2012b, c). For drug treatment, all compounds were dissolved in DMSO at the concentrations noted, and DMSO was the vehicle control in all experiments. Compounds were added every 48 hr during treatment period: γ-secretase inhibitor, DAPT (Sigma); γ-secretase modulator, E2012 (ChemExpress); and β-secretase inhibitor LY2886721 (Selleck).

Immunocytochemistry and Imaging

Fixed and immunostained cultures were imaged on an Olympus FV1000 inverted confocal microscope (see Supplemental Information for details). For

optical clearing, fixed cultures were processed according to the method described (Yang et al., 2014).

Protein Analysis

Quantification of Aβ42, Aβ40, and Aβ38 were carried out with multiplexed MesoScale Discovery assay kits on a Quickplex SQ120 instrument (MesoScale Discovery) using 25 μl of cell culture supernatant. All statistical comparisons were between the entire set of controls samples and all samples of each genotype, using Student's t test with the Bonferroni correction for multiple testing. Three independent cultures of neurons derived from each clone were used for all measurements, except where noted. Cellular protein extraction and western blot analysis were carried out as described (Supplemental Information).

IP-MALDI Analysis of Aβ Peptides

IP of cell media was performed using a KingFisher magnetic particle processor (Thermo Scientific) as described (Portelius et al., 2007). See Supplemental Information for further details.

SUPPLEMENTAL INFORMATION

Supplemental Information includes Supplemental Experimental Procedures, four figures, and two movies and can be found with this article online at http://dx.doi.org/10.1016/j.celrep.2015.03.068.

ACKNOWLEDGMENTS

The authors thank individual donors for providing skin biopsies; Dr. Nathalie Ryan, Prof. Nick Fox, and Prof. Martin Rossor for patient characterization and collection of patient material; Dr. Selina Wray for provision of dermal fibroblasts; Ayiba Momoh and Laura Brightman for technical support; and members of the F.J.L. lab for critical reading of the manuscript. This research was supported by grants from Alzheimer's Research UK and the Wellcome Trust (to F.J.L.) and core funding to the Gurdon Trust from the Wellcome Trust and Cancer Research UK. N.S. was supported by a Woolf-Fisher Trust (NZ) PhD studentship. H.Z. was supported by the Wolfson Centre at UCL, and the UCLH Dementia BRU provided financial support for the collection of patient materials. F.J.L. is a Wellcome Trust Senior Investigator, K.B. is a Torsten Söderberg Academy Professor, and H.Z. is a Wallenberg Academy Fellow.

Received: July 1, 2014
Revised: January 29, 2015
Accepted: March 26, 2015
Published: April 23, 2015

REFERENCES

Benilova, I., Karran, E., and De Strooper, B. (2012). The toxic Aβ oligomer and Alzheimer's disease: an emperor in need of clothes. Nat. Neurosci. *15*, 349–357.

Bertram, L., and Tanzi, R.E. (2008). Thirty years of Alzheimer's disease genetics: the implications of systematic meta-analyses. Nat. Rev. Neurosci. *9*, 768–778.

Blennow, K., de Leon, M.J., and Zetterberg, H. (2006). Alzheimer's disease. Lancet *368*, 387–403.

Chávez-Gutiérrez, L., Bammens, L., Benilova, I., Vandersteen, A., Benurwar, M., Borgers, M., Lismont, S., Zhou, L., Van Cleynenbreugel, S., Esselmann, H., et al. (2012). The mechanism of γ-Secretase dysfunction in familial Alzheimer disease. EMBO J. *31*, 2261–2274.

Choi, S.H., Kim, Y.H., Hebisch, M., Sliwinski, C., Lee, S., D'Avanzo, C., Chen, H., Hooli, B., Asselin, C., Muffat, J., et al. (2014). A three-dimensional human neural cell culture model of Alzheimer's disease. Nature *515*, 274–278.

De Strooper, B. (2010). Proteases and proteolysis in Alzheimer disease: a multifactorial view on the disease process. Physiol. Rev. *90*, 465–494.

Devine, M.J., Ryten, M., Vodicka, P., Thomson, A.J., Burdon, T., Houlden, H., Cavaleri, F., Nagano, M., Drummond, N.J., Taanman, J.W., et al. (2011). Parkinson's disease induced pluripotent stem cells with triplication of the α-synuclein locus. Nat. Commun. *2*, 440.

Glenner, G.G., and Wong, C.W. (1984a). Alzheimer's disease: initial report of the purification and characterization of a novel cerebrovascular amyloid protein. Biochem. Biophys. Res. Commun. *120*, 885–890.

Glenner, G.G., and Wong, C.W. (1984b). Alzheimer's disease and Down's syndrome: sharing of a unique cerebrovascular amyloid fibril protein. Biochem. Biophys. Res. Commun. *122*, 1131–1135.

Hardy, J., and Allsop, D. (1991). Amyloid deposition as the central event in the aetiology of Alzheimer's disease. Trends Pharmacol. Sci. *12*, 383–388.

Hooli, B.V., Kovacs-Vajna, Z.M., Mullin, K., Blumenthal, M.A., Mattheisen, M., Zhang, C., Lange, C., Mohapatra, G., Bertram, L., and Tanzi, R.E. (2014). Rare autosomal copy number variations in early-onset familial Alzheimer's disease. Mol. Psychiatry *19*, 676–681.

Israel, M.A., Yuan, S.H., Bardy, C., Reyna, S.M., Mu, Y., Herrera, C., Hefferan, M.P., Van Gorp, S., Nazor, K.L., Boscolo, F.S., et al. (2012). Probing sporadic and familial Alzheimer's disease using induced pluripotent stem cells. Nature *482*, 216–220.

Lauritzen, I., Pardossi-Piquard, R., Bauer, C., Brigham, E., Abraham, J.-D., Ranaldi, S., Fraser, P., St-George-Hyslop, P., Le Thuc, O., Espin, V., et al. (2012). The β-secretase-derived C-terminal fragment of βAPP, C99, but not Aβ, is a key contributor to early intraneuronal lesions in triple-transgenic mouse hippocampus. J. Neurosci. *32*, 16243–16255a.

Masters, C.L., Simms, G., Weinman, N.A., Multhaup, G., McDonald, B.L., and Beyreuther, K. (1985). Amyloid plaque core protein in Alzheimer disease and Down syndrome. Proc. Natl. Acad. Sci. USA *82*, 4245–4249.

Muratore, C.R., Rice, H.C., Srikanth, P., Callahan, D.G., Shin, T., Benjamin, L.N.P., Walsh, D.M., Selkoe, D.J., and Young-Pearse, T.L. (2014). The familial Alzheimer's disease APPV717I mutation alters APP processing and Tau expression in iPSC-derived neurons. Hum. Mol. Genet. *23*, 3523–3536.

Park, I.H., Arora, N., Huo, H., Maherali, N., Ahfeldt, T., Shimamura, A., Lensch, M.W., Cowan, C., Hochedlinger, K., and Daley, G.Q. (2008). Disease-specific induced pluripotent stem cells. Cell *134*, 877–886.

Pimplikar, S.W., Nixon, R.A., Robakis, N.K., Shen, J., and Tsai, L.-H. (2010). Amyloid-independent mechanisms in Alzheimer's disease pathogenesis. J. Neurosci. *30*, 14946–14954.

Portelius, E., Tran, A.J., Andreasson, U., Persson, R., Brinkmalm, G., Zetterberg, H., Blennow, K., and Westman-Brinkmalm, A. (2007). Characterization of amyloid beta peptides in cerebrospinal fluid by an automated immunoprecipitation procedure followed by mass spectrometry. J. Proteome Res. *6*, 4433–4439.

Portelius, E., Price, E., Brinkmalm, G., Stiteler, M., Olsson, M., Persson, R., Westman-Brinkmalm, A., Zetterberg, H., Simon, A.J., and Blennow, K. (2011). A novel pathway for amyloid precursor protein processing. Neurobiol. Aging *32*, 1090–1098.

Rovelet-Lecrux, A., Hannequin, D., Raux, G., Le Meur, N., Laquerrière, A., Vital, A., Dumanchin, C., Feuillette, S., Brice, A., Vercelletto, M., et al. (2006). APP locus duplication causes autosomal dominant early-onset Alzheimer disease with cerebral amyloid angiopathy. Nat. Genet. *38*, 24–26.

Rovelet-Lecrux, A., Hannequin, D., Guillin, O., Legallic, S., Jurici, S., Wallon, D., Frebourg, T., and Campion, D. (2010). Frontotemporal dementia phenotype associated with MAPT gene duplication. J. Alzheimers Dis. *21*, 897–902.

Shi, Y., Kirwan, P., Smith, J., Maclean, G., Orkin, S.H., and Livesey, F.J. (2012a). A human stem cell model of early Alzheimer's disease pathology in Down syndrome. Sci. Transl. Med. *4*, 124ra29.

Shi, Y., Kirwan, P., Smith, J., Robinson, H.P., and Livesey, F.J. (2012b). Human cerebral cortex development from pluripotent stem cells to functional excitatory synapses. Nat. Neurosci. *15*, 477–486, S1.

Shi, Y., Kirwan, P., and Livesey, F.J. (2012c). Directed differentiation of human pluripotent stem cells to cerebral cortex neurons and neural networks. Nat. Protoc. *7*, 1836–1846.

Takahashi, K., Tanabe, K., Ohnuki, M., Narita, M., Ichisaka, T., Tomoda, K., and Yamanaka, S. (2007). Induction of pluripotent stem cells from adult human fibroblasts by defined factors. Cell *131*, 861–872.

Wray, S., Self, M., Lewis, P.A., Taanman, J.W., Ryan, N.S., Mahoney, C.J., Liang, Y., Devine, M.J., Sheerin, U.M., Houlden, H., et al.; NINDS Parkinson's Disease iPSC Consortium; NINDS Huntington's Disease iPSC Consortium; NINDS ALS iPSC Consortium (2012). Creation of an open-access, mutation-defined fibroblast resource for neurological disease research. PLoS ONE *7*, e43099.

Yagi, T., Ito, D., Okada, Y., Akamatsu, W., Nihei, Y., Yoshizaki, T., Yamanaka, S., Okano, H., and Suzuki, N. (2011). Modeling familial Alzheimer's disease with induced pluripotent stem cells. Hum. Mol. Genet. *20*, 4530–4539.

Yang, B., Treweek, J.B., Kulkarni, R.P., Deverman, B.E., Chen, C.-K., Lubeck, E., Shah, S., Cai, L., and Gradinaru, V. (2014). Single-cell phenotyping within transparent intact tissue through whole-body clearing. Cell *158*, 945–958.

Yankner, B.A., Dawes, L.R., Fisher, S., Villa-Komaroff, L., Oster-Granite, M.L., and Neve, R.L. (1989). Neurotoxicity of a fragment of the amyloid precursor associated with Alzheimer's disease. Science *245*, 417–420.

Cell Reports

Supplemental Information

APP Metabolism Regulates Tau Proteostasis in Human Cerebral Cortex Neurons

Steven Moore, Lewis D.B. Evans, Therese Andersson, Erik Portelius, James Smith, Tatyana B. Dias, Nathalie Saurat, Amelia McGlade, Peter Kirwan, Kaj Blennow, John Hardy, Henrik Zetterberg, and Frederick J. Livesey

APP metabolism regulates tau proteostasis in human cerebral cortex neurons

SUPPLEMENTARY MATERIALS:

1. **Supplementary Methods**
2. **Supplementary Figures**
3. **Supplementary Movies**

SUPPLEMENTARY METHODS

Pluripotent stem cell culture

Pluripotent stem cells were maintained on mouse embryonic fibroblasts (MEFs) (GlobalStem) in DMEM/F12 containing 20% KSR (vol/vol), 100 μm non-essential amino acids, 100 μM 2-mercaptoethanol, 50 U ml^{-1} penicillin and 50 mg ml^{-1} streptomycin (all Life Technologies) and 10 ng ml^{-1} FGF2.

Immunostaining and imaging

Cultures were fixed in 4% paraformaldehyde in phosphate buffered saline or methanol at -20°C before being processed for immunofluorescence staining and confocal microscopy. Antibodies used for immunofluorescence in this study were Tbr1 (Abcam, ab31940), CTIP2 (Abcam, ab18465), β3-tubulin (Covance, MMS-435P), and total tau (Dako Cytomation, A0024).

Calcium imaging

Calcium imaging was performed on familial AD (PSEN1 Y115C, Intron 4 and APPV717) and control (NDC) cultures aged between 8 and 9 weeks post-induction. Cells were loaded with the calcium indicator Oregon Green 488 BAPTA (OGB) by diluting a 0.7mM OGB stock solution to 3.2μM in N2B27 media containing 0.01% v/v Cremaphor EL and 0.4% Pluronic F-127 to make a loading solution. Cells were then bathed in the OGB loading solution for 1 hour at 37ºC and 7% CO_2 in the dark. The loading solution was then removed and the cells were washed over twice with N2B27 and incubated for a further 30 minutes at 37ºC and 7% CO_2 in the dark in N2B27. The cells were then imaged in artificial CSF using a Deltavision (Applied Precision), with an EMCCD camera and using softWoRx 5.0.0 (Applied Precision) software. The imaging chamber was heated to 37ºC and supplied with 5% CO_2. The recordings were 2 minutes in length and were captured at 10 Hz. The 2-minute movies were converted to AVI format playing at 150 frames per second using ImageJ software.

Western blot analysis

Whole cell protein extraction was performed by lysis of cell pellets in cell extraction buffer (Invitrogen) supplemented with PMSF (Sigma), protease inhibitors (Thermo Scientific) and phosphatase inhibitors (Thermo Scientific) before removal of the soluble fraction. Western blot analysis was carried out using the following antibodies: β-actin (Sigma, A2228), β3-tubulin (Covance, MMS-435P), APP C-terminal fragment (Covance, SIG-39152), total tau (Dako Cytomation, A0024), phospho-PHF-tau pS202/T205 - AT8 (Thermo, MN1020), anti-tau Phospho S396 (Abcam, ab109390) and anti-tau Phospho S404 (Abcam, ab92676). Detection of immunoblots was carried out using LI-COR Odyssey CLx Infrared Imaging System and Image Studio Software.

RT-PCR analysis of MAPT transcription

Total RNA was extracted using TRIzol before cDNA was prepared using from 500 ng of RNA superscript II (both Life Technologies). MAPT mRNA expression was assessed using the primer set, forward 5′-AAGTCGCCGTCTTCCGCCAAG-3′; reverse 5′-GTCCAGGGACCCAATCTTCGA-3′ (Iovino et al., 2010). PCR was performed in a final volume of 25 µl using the following protocol. 95°C for 15 min, 30 cycles at 94°C for 30 seconds, 60°C for 30 s and 74 °C for 90 s with a final 10 min extension at 74°C. GAPDH transcription was assessed as a control using the primer set, forward 5' – CTGGTAAAGTGGATATTGTTGCCAT- 3': reverse 5'-TGGAATCATATTGGAACATGTAAACC- 3'. Products were analysed on a 2% agarose gel and imaged with a Molecular Imager Gel Doc XR+ imaging system (BIO RAD)

IP-MALDI analysis of Aβ peptides

For analysis of cell culture media/supernatants, 4 µg of the Aβ-specific antibodies 6E10 and 4G8 (epitope in the N-terminal region and epitope 18-22, respectively, Signet Laboratories, Inc., Dedham, MA, USA) were separately added to 25 µL Dynabeads M-280 (Dynal) sheep anti-mouse according to the manufacturer's product description. Briefly, the IPs were conducted on 940 µL cell media, to which 10 µL 2.5% Tween-20 (Bio-Rad Laboratories Inc.) had been added. The beads/cell media solution (total volume 1 mL) was transferred to a KingFisher magnetic particle processor (polypropylene tubes,

Thermo Scientific) for washing and elution in a 5-step procedure. The collected supernatant was dried in a vacuum centrifuge and redissolved in 5 μL 0.1% formic acid in 20% acetonitrile. Samples were analyzed by MALDI TOF/TOF (Autoflex, Bruker Daltonics, Bremen, Germany) operating in reflector mode. FlexAnalysis (version 3.3, Bruker Daltonics) was used for automated integration of the peaks for each spectrum. Prior to the statistical analysis, the peak areas were normalized to the sum of the integrated peaks, duplicated samples were averaged, and the relative changes compared to baseline values were calculated. All solvents used were of HPLC quality.

REFERENCE:

Iovino, M., Patani, R., Watts, C., Chandran, S., and Spillantini, M.G. (2010). Human stem cell-derived neurons: a system to study human tau function and dysfunction. PLoS ONE *5*, e13947.

SUPPLEMENTARY FIGURES

Figure S1: Derivation and characterisation of *APP* and *PSEN1* mutant iPSC lines

A, B. Reprogrammed fibroblasts from patients with *APP* V717I or *PSEN1* (Y115C, M146I, Intron 4) endogenously express the pluripotency markers Oct3/4, Sox2, Nanog and c-Myc. mRNA expression data normalized to H9 ESC expression levels, error bars = SD. Embryoid body differentiation of each line confirmed pluripotency, assessed by a panel of markers as indicated. Related to **Figure 1A.**

Figure S2: *PSEN1* mutants are hypomorphic loss of function alleles

A-D. Representative IP-MALDI traces demonstrating the increase of Aβ14/15/16 in *PSEN1* mutant neurons compared to control neurons. Quantification of these data was used to generate the statistics presented in Figure 1L and M. **Related to Figure 1K-M.**

Figure S3: Tau proteostasis is altered in fAD neurons

A. Additional technical replicates of the immunoblots for soluble total, pS202/205, pS396 and pS404 tau in fAD and control neurons at day 90 post neural induction, related to **Figure 2A and C.**

B. RT-PCR for *MAPT* demonstrating that the increased tau protein levels observed in *APP* V717I, Ts21 and *APP* (dup) neurons is not a result of increased transcription. GAPDH is included as a control.

Figure S4: Responses of fAD neurons to γ-secretase manipulation

A-C. Quantification of the absolute amounts of Aβ40, Aβ42 and Aβ38 released from fAD neurons, assessed at day 90 post-induction following 20 days of treatment with either DMSO (Ctrl), DAPT (GSI) and E2012 (GSM). **, $p<0.01$, Student's *t*-test. Error bars = SD.

D-F. IP-MALDI analysis of media taken from Ctrl-, GSI- or GSM-treated neurons, demonstrating the efficacy of GSI and GSMs in human neurons.

G-H. Technical replicates of the immunoblots presented in **Figure 4 E-F** for **(G)** total tau and selected phosphorylation sites **(H)** APP-C83/99 and β3-tublin with the respective β-

actin loading control performed on soluble protein extracts of neurons following treatment with the indicated compounds.

Movie S1: fAD cortical progenitors form 3-dimensional neuronal networks

A. 3D rendering of a control neuronal culture at day 100 post induction following tissue clearing and immunostaining for tau (red) and DNA (DAPI, blue). Removal of tau positive neuronal processes reveals the cellular density achieved by this system after months in culture. Z= 145μm. **Related to Figure 1D**.

B. Serial Z sections of control neurons at day 100 post induction following tissue clearing and immunostaining for tau (red) and DNA (DAPI, blue). Z= 118 μm captured in 2 μm steps, scale bar = 62 μm. **Related to Figure 1D**.

Movie S2: fAD neurons form spontaneously active neuronal networks

A-D. Live imaging of neuronal cultures loaded with Oregon Green BAPTA to visualise calcium transients. Control neurons (day 61 post induction, **A**) demonstrate comparable network activity to *PSEN1* intron 4 (day 64 post induction, **B**), *PSEN1* Y115C (day 55 post induction, **C**) and *APP* V717I neurons (day 61 post induction, **D**). **Related to Figure 1A-D.**

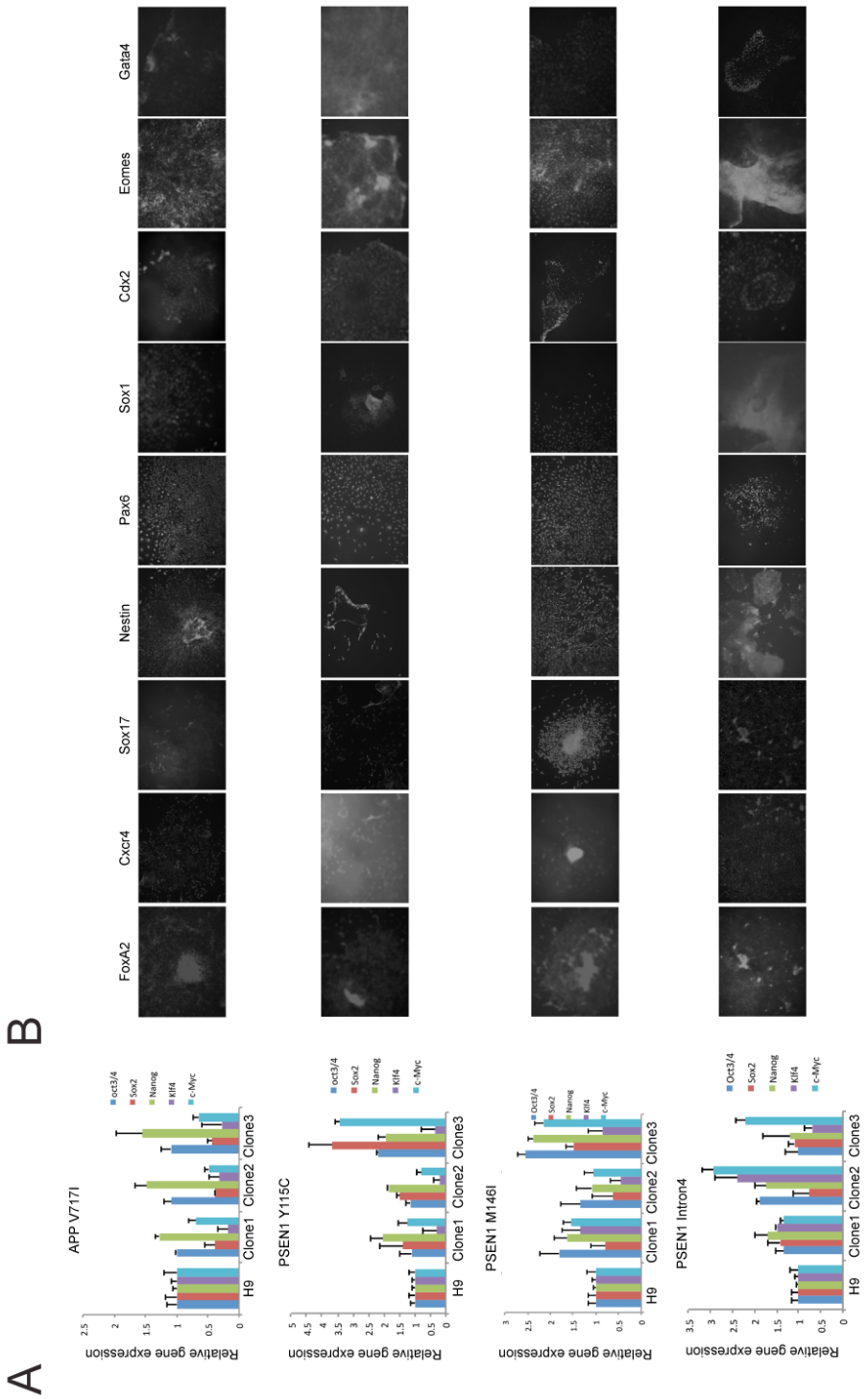
A
B
FoxA2
Cxcr4
Sox17
Nestin
Pax6
Sox1
Cdx2
Eomes
Gata4
APP V717I
PSEN1 Y115C
PSEN1 M146I
PSEN1 Intron4
Oct3/4
Sox2
Nanog
Klf4
c-Myc
Relative gene expression
H9
Clone1
Clone2
Clone3

Figure S1

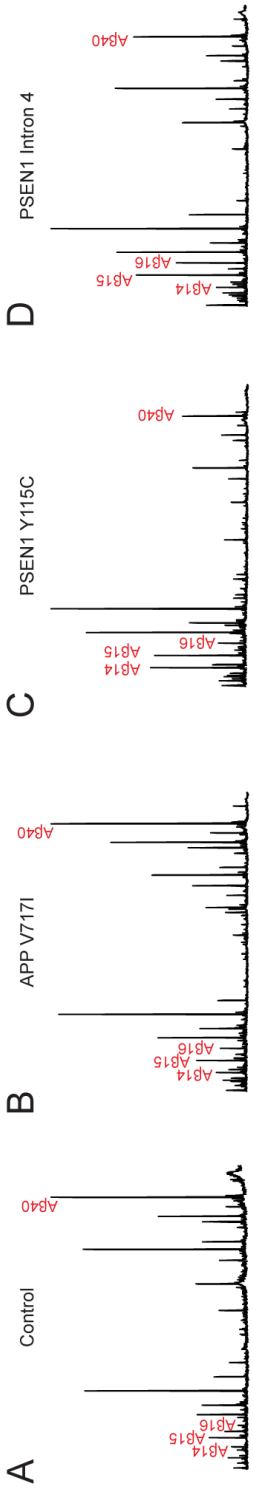
A
Control
Aβ40
Aβ16
Aβ15
Aβ14
B
APP V717I
Aβ40
Aβ16
Aβ15
Aβ14
C
PSEN1 Y115C
Aβ40
Aβ16
Aβ15
Aβ14
D
PSEN1 Intron 4
Aβ40
Aβ16
Aβ15
Aβ14

Figure S2

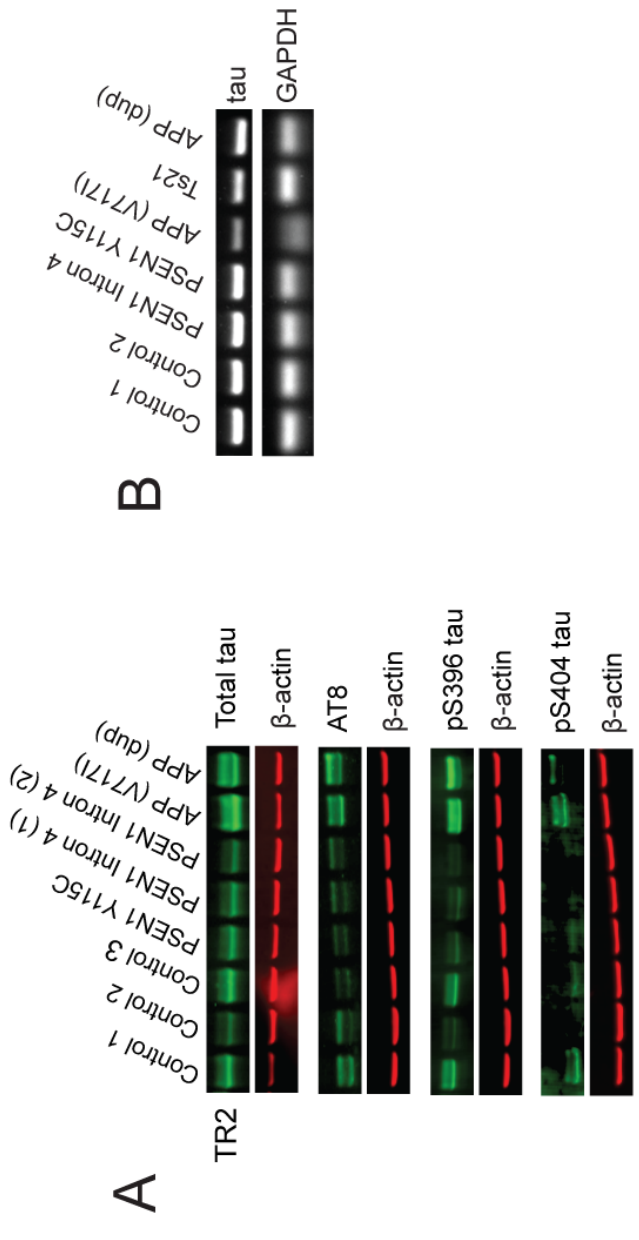
A
TR2
Total tau
β-actin
AT8
β-actin
pS396 tau
β-actin
pS404 tau
β-actin
Control 1
Control 2
Control 3
PSEN1 Y115C
PSEN1 Intron 4 (1)
PSEN1 Intron 4 (2)
APP (V717I)
APP (dup)
B
tau
GAPDH
Control 1
Control 2
PSEN1 Intron 4
PSEN1 Y115C
APP (V717I)
Ts21
APP (dup)

Figure S3

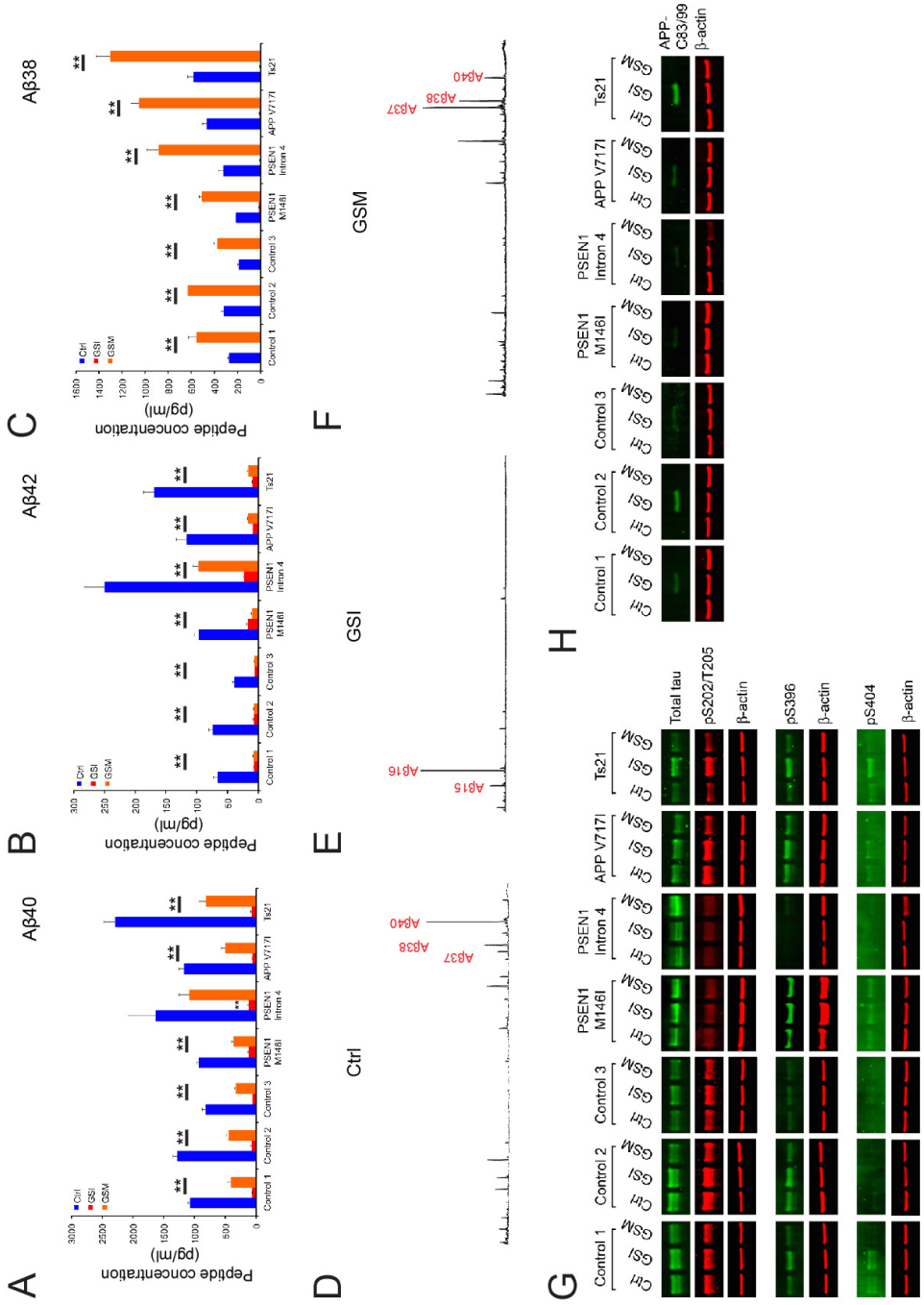
A
Aβ40
Peptide concentration (pg/ml)
Ctrl
GSI
GSM
Control 1
Control 2
Control 3
PSEN1 M146I
PSEN1 Intron 4
APP V717I
Ts21
B
Aβ42
C
Aβ38
D
Ctrl
Aβ37
Aβ38
Aβ40
E
GSI
Aβ15
Aβ16
F
GSM
G
Total tau
pS202/T205
β-actin
pS396
pS404
H
APP-C83/99

Figure S4